

Review

# Cooling of Concentrated Photovoltaic Cells—A Review and the Perspective of Pulsating Flow Cooling

Khalifa Aliyu Ibrahim , Patrick Luk \*  and Zhenhua Luo 

Centre for Energy Engineering, Cranfield University, Cranfield MK43 0AL, UK

\* Correspondence: p.c.k.luk@cranfield.ac.uk

**Abstract:** This article presents a review to provide up-to-date research findings on concentrated photovoltaic (CPV) cooling, explore the key challenges and opportunities, and discuss the limitations. In addition, it provides a vision of a possible future trend and a glimpse of a promising novel approach to CPV cooling based on pulsating flow, in contrast to existing cooling methods. Non-concentrated photovoltaics (PV) have modest efficiency of up to around 20% because they utilise only a narrow spectrum of solar irradiation for electricity conversion. Therefore, recent advances employed multi-junction PV or CPV to widen the irradiation spectrum for conversion. CPV systems concentrate solar irradiation on the cell's surface, producing high solar flux and temperature. The efficient cooling of CPV cells is critical to avoid thermal degradation and ensure optimal performance. Studies have shown that pulsating flow can enhance heat transfer in various engineering applications. The advantage of pulsating flow over steady flow is that it can create additional turbulence and mixing in the fluid, resulting in a higher heat transfer coefficient. Simulation results with experimental validation demonstrate the enhancement of this new cooling approach for future CPV systems. The use of pulsating flow in CPV cooling has shown promising results in improving heat transfer and reducing temperature gradients.

**Keywords:** concentrated solar cell; solar energy; CPV cooling mechanism; electrical and thermal efficiency; high heat flux dissipation; heat transfer enhancement



**Citation:** Ibrahim, K.A.; Luk, P.; Luo, Z. Cooling of Concentrated Photovoltaic Cells—A Review and the Perspective of Pulsating Flow Cooling. *Energies* **2023**, *16*, 2842. <https://doi.org/10.3390/en16062842>

Academic Editors: Luísa Andrade and Vera C.M. Duarte

Received: 10 February 2023

Revised: 16 March 2023

Accepted: 16 March 2023

Published: 18 March 2023



**Copyright:** © 2023 by the authors. Licensee MDPI, Basel, Switzerland. This article is an open access article distributed under the terms and conditions of the Creative Commons Attribution (CC BY) license (<https://creativecommons.org/licenses/by/4.0/>).

## 1. Introduction

Solar energy in the world's total energy mix has become much more significant over the past two decades [1–3]. Photovoltaic (PV) cells produce electricity directly from the sun's irradiation. They are an excellent alternative to decreasing the use of fossil fuels, which contributes to global warming [4–6]. On our planet, solar energy from direct sunlight is both the most widespread and the most easily accessible source of energy [7,8]. Sand, widely accessible globally, is the primary silicon source for PV cells [9]. Most PV systems consist of single-junction PV cells, which have become more cost-effective in recent decades. However, their efficiency is relatively low, around 20%, because they can only convert a narrow range of electromagnetic waves into electricity. Multi-junction PV cells, also known as concentrated photovoltaic (CPV) cells, have recently emerged as an alternative. The structure of multijunction CPV cells broadens the spectrum of electromagnetic waves that can be converted into energy, making them a more attractive option for the renewable energy community. CPV systems utilise equipment such as parabolic mirrors to concentrate and increase solar irradiation density up to 1000 times (1000 suns) at the CPV cell's surface.

In CPV, the electrical and thermal output increases. However, the thermal stresses caused by the concentration make the cell temperature high, which could cause physical damage to the whole system. The current conventional cooling method works based on a continuous flow, which increases the chances of having a non-uniform temperature in CPV. Continuous flow in cooling creates a boundary layer that hinders heat transfer [10]. Pulsating flow may boost heat transfer by disrupting the boundary layer and mixing the fluid [11].

Research shows that pulsating flow enhances heat transfer [12–16]. Most studies report cooling techniques based on a steady, continuous coolant flow. The steady-continuous flow can cause issues with temperature distribution and heat exchange efficiency due to its intrinsic flow dynamic properties. Specifically, it may over-cool the inlet area and under-cool the outlet area, leading to a non-uniform temperature distribution.

This article reviews the existing cooling techniques for concentrated photovoltaics and highlights critical research gaps and findings. The article begins by discussing the classification of photovoltaics and the main challenges and limitations of CPV cooling. It then introduces an innovative approach based on discontinued flow (pulsation flow) as a potential approach and future trend of CPV cooling.

## 2. Photovoltaics Current State of the Art

### 2.1. Classifications

Photovoltaics can be classified as first-generation (1st G), second-generation (2nd G), and third-generation (3rd G), as shown in Figure 1. The 1stG includes monocrystalline panels, polycrystalline panels, and amorphous solar cells. This photovoltaic was the first commercial photovoltaic cell introduced in 1954. In the 21st century, they are the most available solar cell used in residential areas, making up about 80% of the solar cells sold. 1st G can have an efficiency of up to 26% for monocrystalline and 21% for polycrystalline. It is made of silicon and has a bandgap of 1.1 eV [9,17].

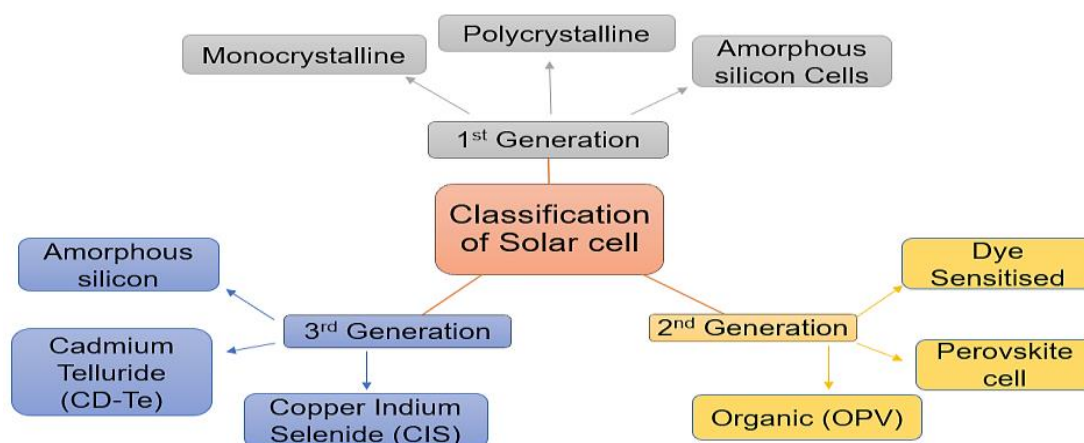


**Figure 1.** Classification of photovoltaic. The 2nd G, with an efficiency of 21.4%, came into existence after 20 years of research and development [9]. The disadvantage of 2nd G is that most of the components of these cells are becoming increasingly rare and expensive (indium), and some are toxic (cadmium). The 3rd G is a recent generation that has emerged due to the high costs of 1st G solar cells, materials availability limitations, and the toxicity of 2nd G solar cells. In addition to silicon, researchers use various new materials to make solar cells, such as nano-materials, silicon wires, solar inks created with conventional printing press technology, conductive plastics, and organic dyes- [9,18]. In [18], the fourth generation (4th G) classifies the new generation of solar cell technology. It uses a combination of organic and inorganic materials for manufacturing. The advantage of 4th G is combining inorganic and organic materials to maintain cost and increase solar to electrical energy conversion efficiency. The maximum efficiency of laboratory-based photovoltaic cells is more than 40%, according to the National Renewable Energy Laboratory (NREL) in 2020 [6]. According to NREL, Figure 2 shows the efficiency improvement trends as of November 2021.

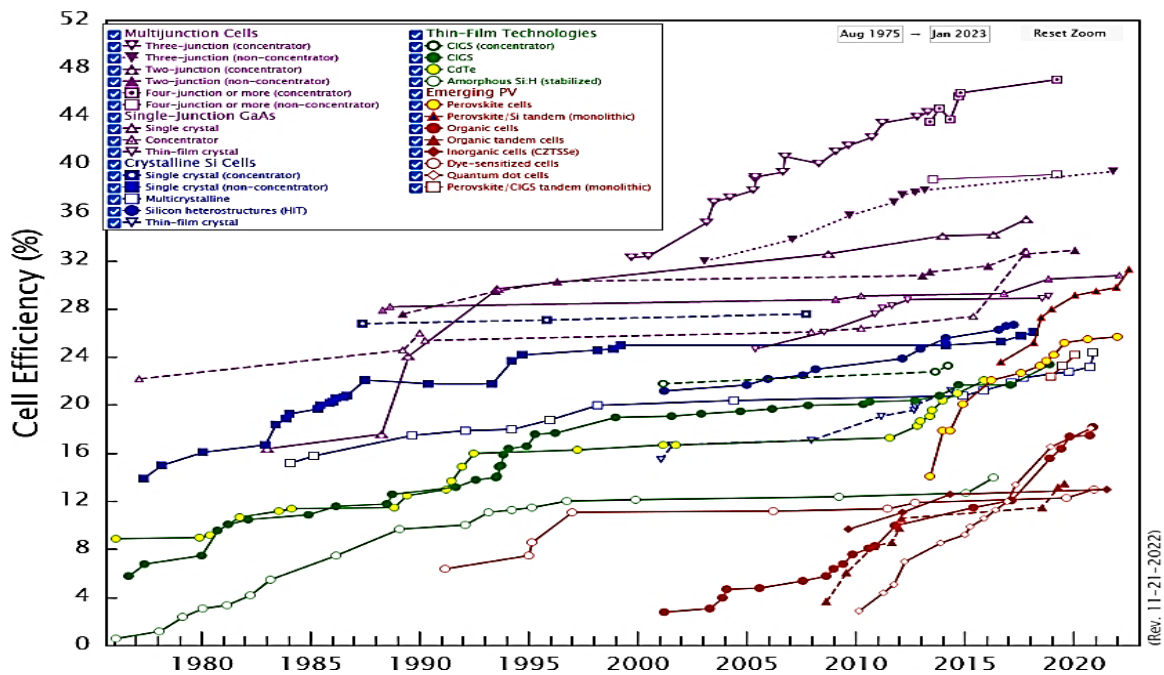


Figure 2. Improvement trends of efficiencies of best laboratory-based solar cells since 1975.

2.2. Concentrated Photovoltaic Cooling

Concentrated photovoltaic (CPV) technologies are new advanced PV systems. The principle of operation includes focusing the sun into a solar cell using reflectors such as mirrors or an optical prism [19–21]. Beams of sun radiation hit a reflector and concentrate the rays of the beam onto a solar cell (Figure 3). A reflector is mostly a mirror or a lens that receives the primary solar radiation from the sun and focuses secondary solar radiation onto a cell located at the reflector’s focal point. CPV systems must track the sun to maintain the radiation’s concentration on the solar panel [22]. With 1000 suns of solar concentration ratio, researchers projected that the temperature of an uncooled solar cell would rise by 1360 °C [19]. Concentrated multijunction solar cells are essential in realising a more efficient photovoltaic. The incident solar energy on the solar cell’s surface is converted to generate electricity. In contrast, the rest is thermally absorbed within the solar cell. Consequently, this increases solar cell temperature [23]. On a long-term basis, increasing panel temperature leads to decreased conversion efficiency and lower panel reliability. Numerous cooling systems are developed and studied to prevent excessive temperature increases and improve their efficiency effectively [7]. As such, the cooling of CPV is still a challenge to researchers.

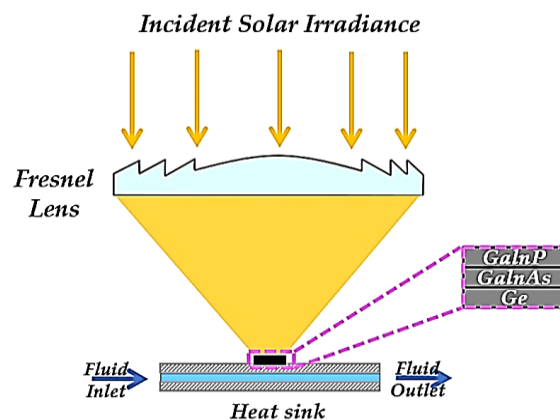
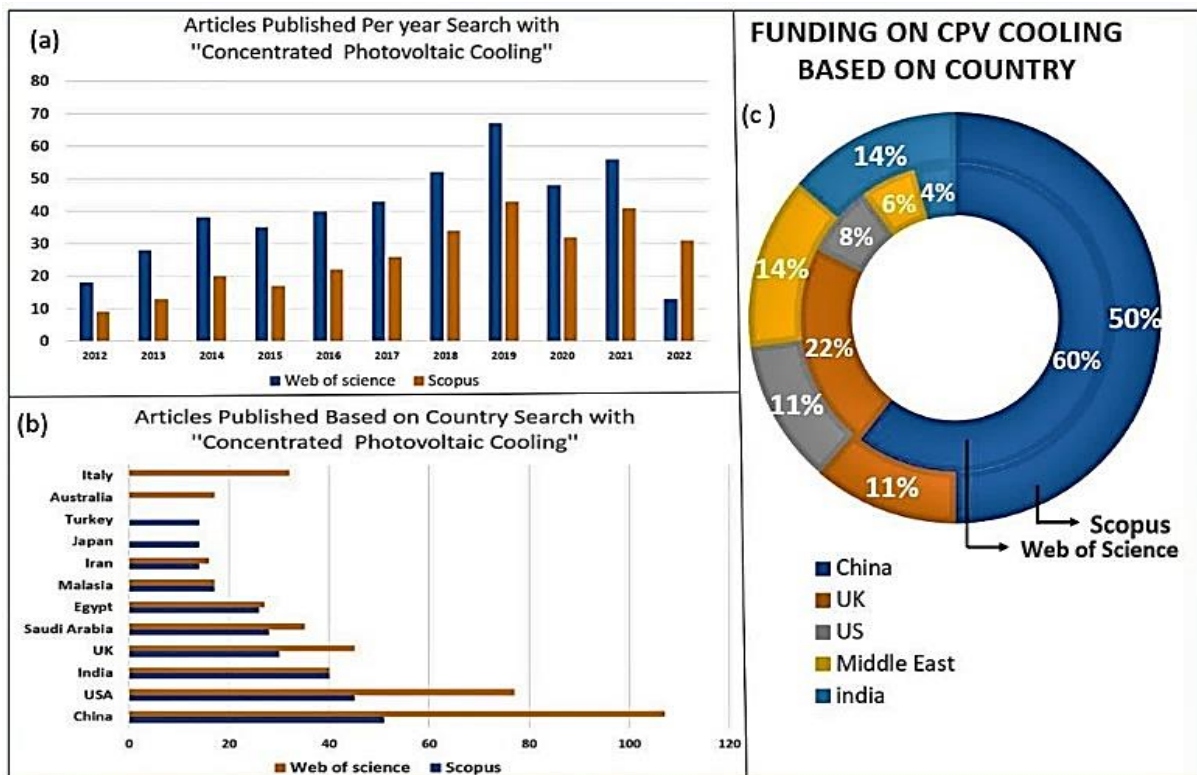


Figure 3. Concentrated photovoltaic [23].

Substantial research on concentrated photovoltaic cooling (CPVC) is ongoing globally. Statistics over the previous decade (2012–2022) show the rising interest and the relevance of CPV cooling technology. In the past decade, researchers have published many research publications. Based on data from the Scopus and Web of Science databases, a search for “Concentrated Photovoltaic Cooling” has yielded over 288 and 438 research papers on CPVC from 2012 to May 2022, respectively. Figure 4 presents a statistical breakdown of research publications on CPVC over the past decade, including the annual number of papers published (Figure 4a), detailed information on the top ten nations with the most significant proportion of research papers (Figure 4b), and the first five countries with the most funding investment (Figure 4c) on this topic.



**Figure 4.** Statistical charts of articles published on CPV cooling. (a) Articles published per year, (b) Articles published based on countries, (c) First five countries with founding investment.

### 3. Types and Classification of Cooling Techniques in Solar Cells

Research by [22] examines the cooling system using an active cooling system pump. It collects the heat from the PV and dissipates it utilising a convector or heat sink. Several researchers have highlighted that active cooling is more efficient and suitable for high concentrations. The authors of [22] experimented and reported that the output of a concentration solar panel is between 4.7 and 5.2 times that of the nonconcentrated cell. The results demonstrate that the solar cell temperature was reduced to below 60 °C, generating more electrical output. Research using parabolic concentrators to analyse heat transfer in photovoltaics has been conducted by [24]. Researchers found that the temperature of the concentrator aperture and the PV cell increased with the intensity of incident solar energy. We have presented a comparative analysis in Table 1 between the most commercially available photovoltaic and a concentrated multijunction solar cell based on the following references [25–30].



**Table 1.** Comparison between primarily used solar cells with concentrated multijunction solar cells.



Type of Solar Cell	Monocrystalline	Polycrystalline	Thin Film	Multi-Junction
Type of Material	Fragments from single wafer crystal	Fragments from different silicon crystals	Fragments from single wafer crystal	Combination of different semiconductors
Life Span	25 to 30 years	20 to 25 years	10 to 20 years	30 or more years
Efficiency	14 to 26%	12 to 21%	Very low	33.8 to 69.1
Appearance	Aesthetic	Non-aesthetic	Aesthetic	Aesthetic
Portability	Big, comes in different size	Big, comes in different size	Flexible lightweight	Lightweight, smaller size
Number of Junctions	1	1	1	It can have 2–7
Cost	High	High	Low	Higher

Research and development in CPV have highlighted the importance of effective cooling. The cooling system ensures that the cell operates within its optimal temperature. CPV cooling design typically has thermal resistance coefficients with good cell temperature uniformity for maximum efficiency [31]. Additionally, it is vital to consider the cooling system's power consumption, ease of installation, and high level of dependability. The selection of a cooling technique depends on the objective and operational environment [31]. However, the suitability of a cooling method is contingent on the solar concentration, location, installation, and system output requirements [32]. Researchers classify CPV cooling as either passive or active, depending on the geometry, coolant, and level of solar concentration [32]. Furthermore, CPV cooling can be categorised based on the nature of heat transfer, natural circulation and forced circulation, or the type of coolant as passive cooling and active cooling [7,33,34]. Researchers report that passive cooling is suitable for concentrations of less than 20 suns; in high concentrations, active cooling is necessary [35].

Natural circulation and forced circulation can be air-based cooling or water-based cooling. Air-based cooling is simple and cheaper [34]. However, it has a lower heat transfer coefficient which varies from 1–10 W/m<sup>2</sup>.K for natural circulation to 20–100 W/m<sup>2</sup>.K for forced circulation [31]. Water-based cooling has a better heat transfer coefficient of 200–1000 W/m<sup>2</sup>.K for natural circulation and 1000–1500 W/m<sup>2</sup>.K for forced circulation [24,36,37]. Ref. [38] stated heat pipe heat sink dissipates flux in CPV. Researchers reported that under 25 suns, the heat pipe and heat sink could cool CPV to 37.8 °C and 54.16 °C, respectively. They have highlighted that this cooling method is cost-effective due to its low energy consumption. The disadvantage of passive cooling is the size in terms of the heatsink area. Economically, the passive system is not viable because it requires a large amount of material, consisting of larger fins and plate areas depending on the concentration ratio [1–3,32,39,40]. Photovoltaic (PV) cells produce electricity directly from the sun's irradiation. They are an excellent alternative to decreasing the use of fossil fuels, which contributes to global warming [4–6]. On our planet, solar energy from direct sunlight is both the most widespread and the most easily accessible source of energy [7,32,39–41]. In other words, the greater the concentration ratio of the CPV, the larger the required heatsink. This has reduced the feasibility and attractiveness of using a PC system to cool a CPV. The use of active cooling (AC) to achieve temperature uniformity has been studied. With this method, the coolant circulates through the cooling system using an active cooling system pump. It collects the heat from the PV and dissipates it utilising a convector or heat sink. Several researchers have highlighted that active cooling is more efficient and suitable for high concentrations [19,38,42,43]. However, one of the limitations posed by AC includes temperature non-uniformity. Table 2 summarises research availability and current challenges of CPV cooling.







**Table 2.** Limitations and challenges in existing methods of CPV cooling.





Cooling Technique	Method of Study	Concentration	Main Challenges	Reference
Heat Pipe and Fins	Experiment	Lower Medium High *	Overheating, uncontrollable oscillatory thermal flows, reverse thermal flows, area-dependent cooling capacity, temperature non-uniformity	[31,32,44–49]
	Theoretical			
	Numerically			
	Simulation			
PCM	Experiment	Lower Medium High *	Limited cooling capacity at higher concentrations, limited amounts of heat energy storage, acidic nature, issue of disposal after lifetime used, mass/weight cooling capacity dependant	[42,50–54]
	Theoretical			
	Numerically			
	Simulation			
Jet Impingement	Experiment	Lower Medium High	System design complexity, draining spent flow, temperature non-uniformity, manufacturing costs	[55–58]
	Theoretical			
	Numerically			
	Simulation			
Immersion Liquid	Experiment	Lower Medium High	Salt deposition issue, cell performance depression, pressure drop, type of liquid, increased weight, design architecture	[42,59–64]
	Theoretical			
	Numerically			
	Simulation			
Microchannel	Experiment	Lower Medium High	Pressure drops, corrosion, temperature non-uniformity, higher manufacturing costs, more power requirements, more studies are needed to commercialise	[65–70]
	Theoretical			
	Numerically			
	Simulation			

Level of Research Reported in CPV cooling:  = Good number of study available;  = Limited number of study available; Level of Concentration (C): *Lower*:  $C < 20$  suns, *Medium*:  $20 < C < 100$ , *High*:  $C > 100$ . \* With a hybrid system configuration.

In order to improve the thermal performance of a system, nanofluids offer a promising solution. However, they have limitations, including high costs, potential corrosion problems, pressure drops, sedimentation, and agglomeration. Hybrid CPV technology, which utilises methods such as jet impingement cooling, microchannels or impingement cooling, and heat pipes, can potentially enhance electrical and thermal performance. Researchers can utilise the organic Rankine cycle (ORC) to create a mutually beneficial scenario to achieve cell temperature reduction while enhancing system output by incorporating a heat recovery system into a CPV thermal system. However, various restrictions and challenges exist associated with implementing concentrated photovoltaic/thermal (CPV/T) hybrid systems, such as complexities related to design, initial costs, component compatibility, and a lack of available platforms integrated model packages for research purposes. Electroosmotic flow (EOF) is another method of improving heat transfer by inducing fluid motion through an electric field, enhancing convective heat transfer [71–73]. This approach can be beneficial in microfluidic channels and other critical applications. Researchers use magnetohydrodynamics (MHD) flow to enhance heat transfer. Applying an external magnetic field induces fluid motion and enhances convective heat transfer. MHD flow has been used in various heat transfer applications, such as nuclear reactors, liquid metal batteries, and plasma devices [70–72]. The limitations and research gaps of the current approach to heat transfer enhancement are summarised in Table 3.

**Table 3.** Heat transfer enhancement approach in thermal energy management (MHTE).

MHTE Approach	Area of Approach	Current State of Art	Research Gap and Limitations
Use of Nanofluid	Type coolant		Corrosion problems, stability issues, sedimentation issues, agglomeration issues, pressure drop, high cost
Hybrid Cooling	Overall system		Compatibility issues, cost economic viability, integrating components within a single system
Boiling Heat Pipes (PHP)	Phase change liquids		Limited modelling tools, no flow pattern control, little experimental work, and availability of components to measure flow.
Magneto Hydrodynamics (MHD)	Type coolant and overall system		Limited experimental work, more numerical models and simulations research are required, and additional cost
Electro Osmotic Flow (EOF)	Porous material under the influence of an electric field		Limited modelling tools, effects of channel geometries on the EOF, design optimisation
Pulsating Flow	Flow and overall system		Limited theoretical study, more research is needed combined with porous media, contradicting results, additional cost due to using of solenoid valves, other means to provide pulsation can be explored, may lead to system complexity

Level of Research Reported:  = Applied to CPV cooling, and a good number of studies are available;  = Good number of studies available with limited research in a ground couple/ ORC systems;  = Limited number of studies available and have been in the field of electronics;  = Studies available mainly in the field of medicine, electronics, and mechanical engineering but has not been applied to CPV cooling.

Numerous studies have emphasised the benefits of pulsating for improving cooling. This article suggests exploring the potential of unsteady flow for CPV cooling performance instead of relying on continuous flow. Valves integrated with controls and sensors can achieve this. One promising method to enhance thermal performance is nanofluids. However, limitations include high cost, corrosion problems, pressure drop, sedimentation, and agglomeration. Formal research has been conducted on hybrid CPV technology to improve electrical and thermal performance. A hybrid system incorporating jet impingement cooling, microchannels or impingement cooling, and heat pipes can facilitate high heat dissipation rates in robust systems. Integrating a heat recovery system into a CPV thermal system can further increase the capabilities of CPV cooling, with the organic Rankine cycle providing a means to maximise waste heat utilisation and create a win-win situation between cell temperature reduction and system output enhancement. The design and implementation of concentrated photovoltaic/thermal (CPV/T) hybrid systems present several challenges and restrictions. These include incorporating two or more methods, higher initial costs than conventional power systems, compatibility issues between components, and a lack of platforms and integrated model packages for investigating different hybrid systems to minimise experiment costs and errors.

#### 4. Pulsating Flow on CPV Cooling

The literature reviewed in this article shows that CPV systems deal with the challenging task of maintaining cell temperature. Concentrating solar energy on a solar cell results in an increase in both electrical and thermal output. However, the high temperature resulting from the concentration causes thermal stresses on the cell, which can physically damage the entire system. The CPV needs an excellent cooling mechanism to have a higher net output power and run reliably. Several research studies highlighted concentrated solar cell temperature non-uniformity resulting in hot regions and cooled spots that need further

study. The current conventional cooling method works based on a continuous flow, which increases the chances of having a non-uniform temperature in CPV. Another challenge researchers face is the continuous fluctuation of solar radiation intensity caused by uncontrollable conditions such as clouds. This poses a particular problem as the environment changes depending on the weather.

Using two-phase liquid to enhance heat transfer, heat pipe pulsating technology has been used in electronic devices and electrical components. It was introduced in the 1990s as an oscillating heat pipe [74]. Ref. [75] reported that pulsating heat pipes are applied for cooling electronic equipment within a short distance or where space is relatively compact. Researchers suggested that the heat pipe is filled with a fraction of 40–60% of heat transfer working liquid in a small capillary tube diameter [75–77]. The phase change liquid boils or evaporates, causing pressure increase in the section where heat is applied. Due to the pressure difference, the vapour in the heating section moves to the liquid cooling section, and the liquid cooling moves to the heating section (Figure 5). These processes continue to happen, making the liquid in the tube continuously oscillate. The process generates a pulsating flow within the two sections of the tube, resulting in reduced weight due to the requirement of a smaller fraction of liquid and air within the tube and the ability to function with a smaller diameter [75]. Pulsating heat pipes (PHP) are an emerging subject of study to researchers, with dozens of articles published yearly. However, limited knowledge of their performance and a lack of scientific modelling tools restricts practical application [76].

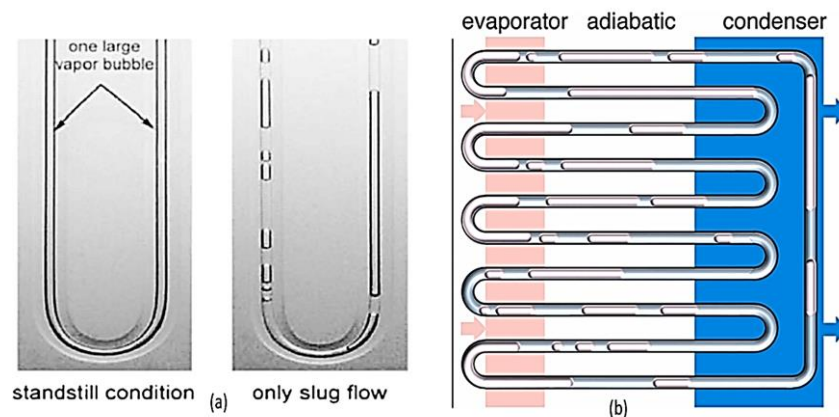


**Figure 5.** Looped pulsating heat pipe (a) Glass showing fluid and air [78] (b) Process diagram adapted from [76].

Researchers have demonstrated that the flow pattern within PHPs switches from an oscillatory pattern to a circulation pattern, ultimately enhancing overall thermal performance. Ref. [79] carried out an experiment using a high-speed camera to visualisation PHP flow. An increase in the channel's inner diameter was reported to shift the flow pattern to a circular form from an oscillatory pattern, which correlates with increased thermal performance. Several researchers have reported that shifting pulsating flow to circular flow increases the basis and enhances thermal performance. Additionally, circular flow helps vapour plugs from the evaporation section to recirculate more [79–83].

Continuous flow in cooling creates a boundary layer which hinders heat transfer [10]. Pulsating flow may boost heat transfer by disrupting the boundary layer and mixing the fluid [11]. Pulsation flow is transient, which adds complexity to the analytical investigation [84,85]. Many modelling and computational fluid dynamics studies are available in the literature. However, little experimental work exists due to inadequate technology to measure pulsating properties. Velocity measurement is more challenging in pulsed flow than in continuous steady flow. However, with research and development, technology has improved to address those challenges [85]. Another challenge is that flowmeters cannot record the exact results at high frequencies due to their weak reaction time. Temperature prediction is also challenging [85]. Important parameters to consider in pulsating flow

include frequency, amplitude, axial position, relaxation time, pulsation source, Womersley number, Reynolds number, distance, and Nusselt and Prandtl numbers all impact heat transfer in pulsating flow [86]. Ref. [87] reported that transient heat flux in CPV leads to flow regularly boiling in microchannels. More work is needed to address the lack of control parameters in boiling and irregular oscillation, which still pose a challenge in boiling and PHPs. With current research and development, using valves to control the nature of the oscillation is an area to explore.

Based on the literature search, cooling with direct couple pulsations has not been applied to CPV cooling. Researchers working around CPV cooling can consider integrating pulsating flow into the existing CPC cooling techniques to enhance heat transfer. Some articles that provide detailed information on pulsation flow include [77,78,78,80,88–90]. The correlations for continuous and pulsating flow are as follows; in a continuous flow, the Reynolds number ( $Re$ ) is a parameter that differentiates between turbulent flow and laminar flow. It is given by Equation (1) where  $D_h$  is the hydraulic diameter,  $\rho$  is the density,  $\mu$  is the dynamic viscosity,  $v$  is the velocity, and  $\nu$  represents kinematic viscosity.

$$Re = \frac{\rho v D_h}{\mu} = \frac{v D_h}{\nu} \quad (1)$$

Nusselt number ( $Nu$ ) is the ratio of the heat transferred by convection and the hydraulic diameter to the thermal conductivity of the coolant, in this case, water.  $h$  is the heat transfer coefficient,  $k$  is the thermal conductivity.

$$Nu = \frac{h D_h}{k} \quad (2)$$

The heat transfer coefficient was calculated using Equation (3) according to [91,92], where  $m$  is the mass flow rate,  $c_p$  is the specific heat capacity,  $T_{out}$  and  $T_{in}$  are the fluid inlet and outlet temperature, and  $T_s$  and  $T_f$  are the cooling pad temperature and average fluid temperature, respectively.

$$h = \frac{m c_p (T_{out} - T_{in})}{A (T_s - T_f)} \quad (3)$$

Equation (4) provides the pressure drop as a function of the friction factor, where for a smooth rectangular channel, the friction function  $f = 68.34/Re$  for lamina flow, and  $f = 0.31/Re^{0.25}$  for turbulent flow, according to [93].

$$\Delta P = f \times \frac{l}{D_h} \times \frac{v^2}{2} \times \rho \quad (4)$$

In pulsating flow, Equation (5) gives the Reynolds number associated with the oscillating  $Re_\omega$  and the stable components  $Re_s$  [90]. The pulsating velocity is given by  $u_s = v(1 + k \sin \omega t)$ ,  $k = 2\pi f A_0/v$  refers to as waviness of the flow, where  $v$  is the average velocity [94],  $A_0 = u_s D_h/v$  [95],  $f = 1/T$  is the frequency of pulsation, and  $T = T_1 + T_2$  is the period where  $T_1$  and  $T_2$  are the first and second-half periods of pulsating [96].

$$Re_\omega = \frac{A_0^2}{\nu \omega}, \quad Re_s = \frac{u_s D_h}{v} \quad (5)$$

In pulsating flow, the Nusselt number is considered a time average. The Nusselt number is used to determine the heat transmission properties. Equations (6) and (7) give the expression according to [90] and [13], respectively. Equation (8) calculates the degree of heat transfer enhancement ( $E$ ), with  $N_p$  referring to the pulsating average Nusselt number, and  $N_{np}$  referring to the non-pulsating Nusselt number [94].

$$Nu = \int_0^L \int_0^T Nu(x, t) dt dx \quad (6)$$



$$Nu = \frac{hD_h}{k_f} \quad (7)$$

$$E = \frac{N_p}{N_{np}} \quad (8)$$

The heat transfer coefficient is given by Equation (9) as a function of the mean log temperature where  $Q = mc_p(T_{out} - T_{in})$ , and  $A_s$  It is the heat transfer area.

$$h = \frac{Q}{A_s(\Delta T_{LMT})} = \frac{Q}{A_s \left[ \frac{(T_s - T_{in}) - (T_s - T_{out})}{\ln \left( \frac{T_s - T_{in}}{T_s - T_{out}} \right)} \right]} \quad (9)$$

In an oscillating flow, the Womersley number expresses the influence of frequency on which force, inertia, or viscosity will dominate. It is given by Equations (10) or (11), according to [90]

$$\alpha = L \left( \frac{\omega}{\nu} \right)^{1/2} \quad (10)$$

$$\alpha = (2\pi ReSt)^{1/2} \quad (11)$$

The Strouhal number is another dimensionless number used in a pulsating flow, according to [90]. It is used to express the frequency divided by the velocity as Equation (12).

$$St = \frac{fL}{u} \quad (12)$$

The pressure drops can be expressed as Equation (13) for  $\alpha < 1$  or Equation (14).

$$\Delta P = \frac{8\mu L Q}{\pi R^4} \quad (13)$$

$$\Delta P = f\rho \left( \frac{l}{D_h} \right) \left( \frac{v^2}{2} \right) \quad (14)$$

## 5. Novel Approach to CPV Cooling

Research shows that pulsating flow enhances heat transfer [12–16]. In this section, a 3D model was developed to study the feasibility of applying pulsating flow to CPV using computational fluid dynamics. We designed the model using SOLIDWORKS and conducted the analysis using Ansys FLUENT software. The design specifications for both the simulation and experiment are presented in the Table 4.

**Table 4.** Model design specifications.

Parameter	Parameter	Design Specification	Hydraulic Diameter ( $D_h$ )
Circular Section	Circular inlet diameter (m)	0.0085	0.0085
	Inlet radius (m)	0.00425	
	Cross-section area (m <sup>2</sup> )	0.000056752	
Actual Channel Section	Inlet channel area (m <sup>2</sup> )	0.00007225	0.00544
	Actual channel area (m <sup>2</sup> )	0.000034	
Multi Junction Solar Cell	Channel length (m)	0.4	
	Single solar cell length (m)	0.01	
	Single solar cell width (m)	0.010275	
	Single solar cell area (m <sup>2</sup> )	0.00010275	

Figure 6 shows the model design considering the use of water as a coolant. Figure 6a shows the channel view, while Figure 6b shows the coupled design with the solar cell. Germanium material was used as the solar cell, while aluminium was used as the cooling pad material. A combination of the laminar model corresponding to a Reynolds number ( $Re$ ) of 1482.41 at 0.5 L/m and an enhanced wall function  $K$ - $\epsilon$  model corresponding to 1–2.5 L/m with an increase in  $Re$  from 1482.41 to 8372.26 was used and adapted, as described in [97–101]. A  $10^{-6}$  residual was considered to indicate a converged solution. A total heat flux of  $150,000 \text{ W/m}^2$ , equivalent to a concentration of 150 suns of the solar simulator used for the experiment, was applied. The complete 3D model (Figure 6c) was constructed using a three-axis computer numerical control (CNC) machine with flat plate material made of Aluminium 6082T6 manufacture by Ooznest UK. The pulsating flow was generated using an Arduino MEGA microcontroller sourced through RS components UK, integrated with a solenoid valve, which opened and closed at a frequency of 0.5 Hz and a period of 2 s. A 5-multijunction solar cell was used.

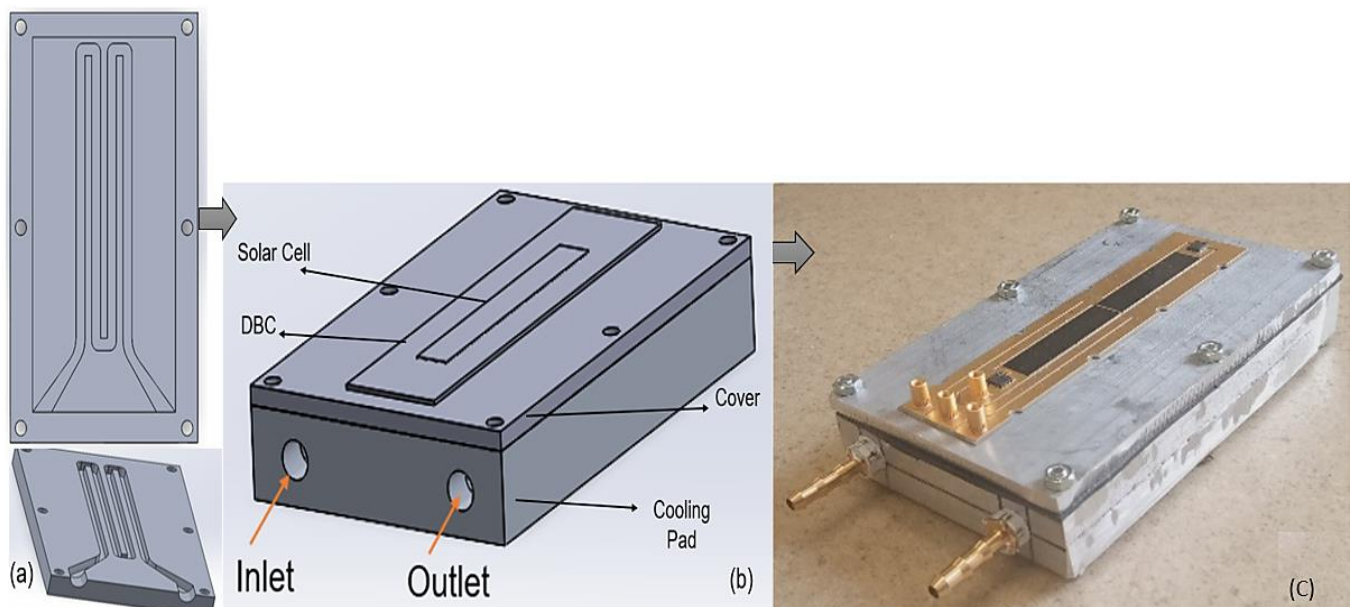


**Figure 6.** Model (a) Channel view (b) Complete coupled design used for simulation (c) Built model design used for the experiment.

A mesh sensitivity analysis was conducted by increasing the number of cells until the  $y^+$  value was less than zero, as shown in Figure 7. The mesh used for the analysis consisted of 7,102,996 cells and 1,416,393 nodes with a  $Y^+$  value of 0.765. A user-defined function (UDF) was created for a flow rate ranging from 0.5 L/m (0.0085 kg/s) to 2.5 L/m (0.0425 kg/s) to generate pulsating flow at the inlet. The equivalent flow rate velocity (ranging from 0.5 L/m to 2.5 L/m) was used in the UDF, which was then imported into the FLUENT software. Subsequently, boundary conditions were defined at the walls, inlet, and outlet. The experimental process flow adopted is illustrated in Figure 8. Finally, a high-flux sun simulator experiment was conducted to validate the model.

The experimental setup is shown in Figure 9, which was built using a high-flux concentrated sun simulator. In a series, two large radiators connected with a fan were used as the heat sink. The simulator was turned ON for 10 min, after which the shutter was opened to concentrate the light on the cell. The cooling system was then turned ON for 5 min to stabilise the cell's concentration. The experiment was conducted for 25 min, with a fixed flow rate ranging from 0.5 L/m to 2.5 L/m, the same as the simulation. Data were recorded every minute, and the average of the recorded data after 5 min was exported to a spreadsheet and used for further analysis. The solar cell's maximum theoretically required cooling capacity was 823 W.

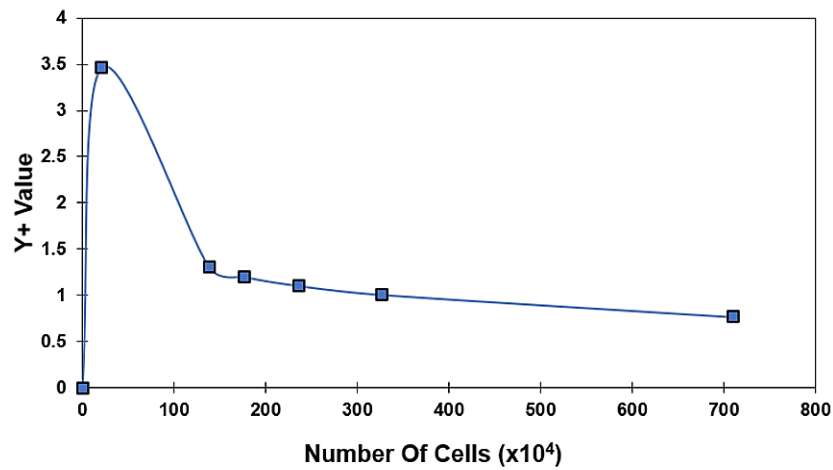


Figure 7. Model mesh sensitivity analysis.

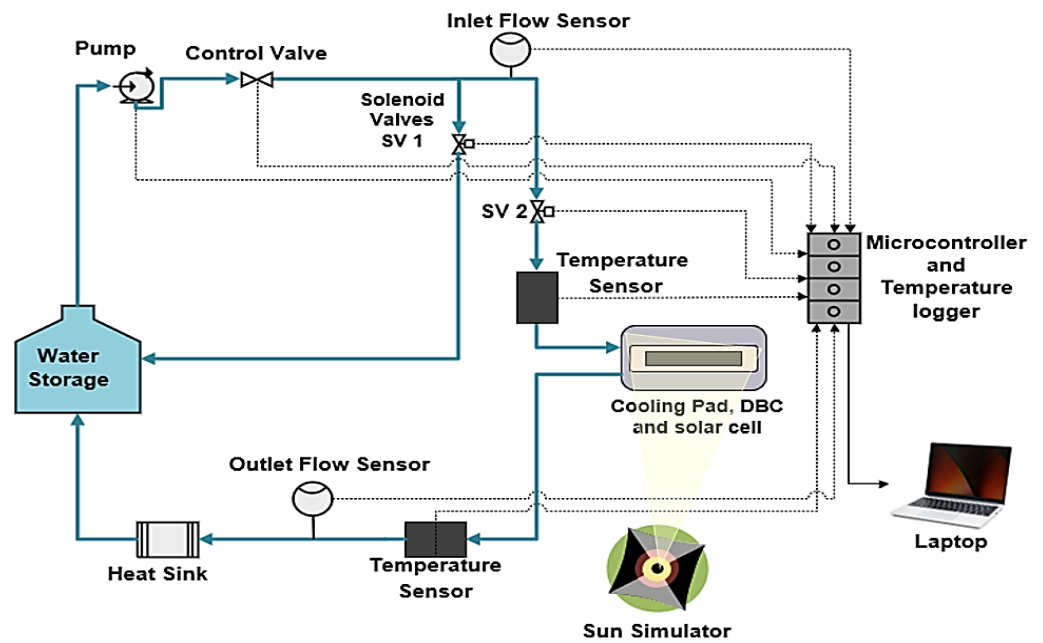


Figure 8. Experimental process flow diagram.

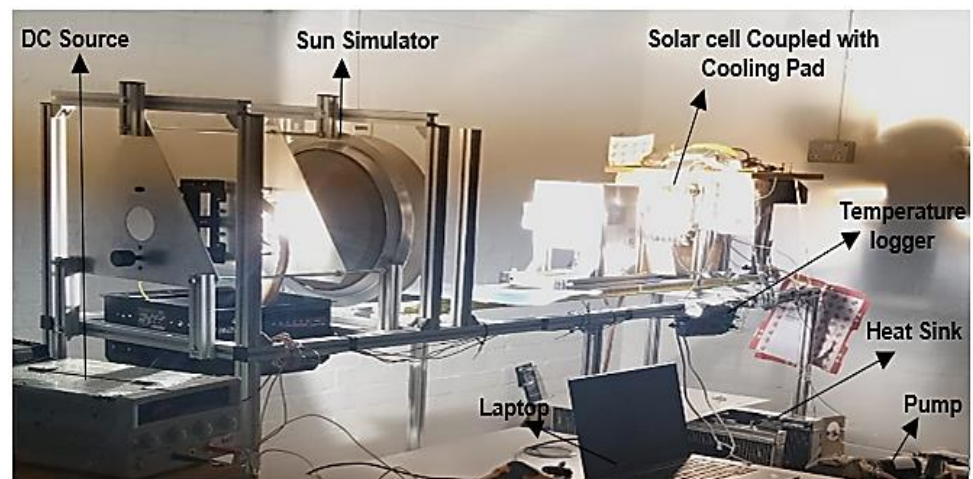


Figure 9. Experimental setup.

5.1. Simulation Results

Figure 10 shows the temperature contour of the solar cell for both continuous flow and pulsating flow at 1 L/m. The pulsating flow, with a period of 2 s and a frequency of 0.5 Hz, equivalent to 30 pulses/minute (Figure 9b), exhibited better cooling than the continuous flow (Figure 9a), with a maximum and minimum temperature interval of 298 K to 308 K.

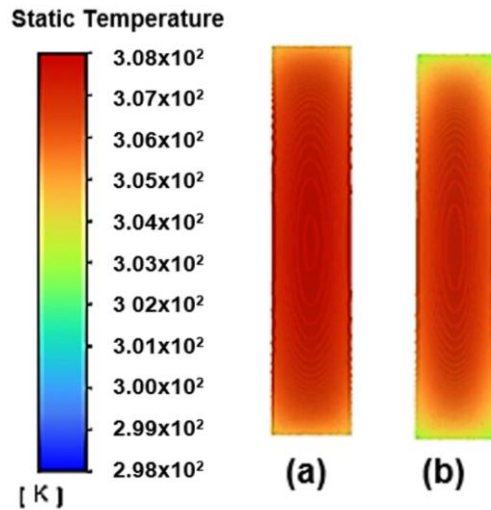


Figure 10. Temperature contour of solar cell from simulation (a) Continuous flow (b) Pulsating flow at 30 pulse/minute.

Figure 11 shows the model’s 2 D x-y centre-cut view temperature contour for continuous and pulsating flow at 1 L/m, with a maximum and minimum temperature interval of 298 K to 308 K. The pulsating flow, with a period of 2 s and a frequency of 0.5 Hz, equivalent to 30 pulses/minute (Figure 10b), shows better cooling compared to continuous flow (Figure 10a).

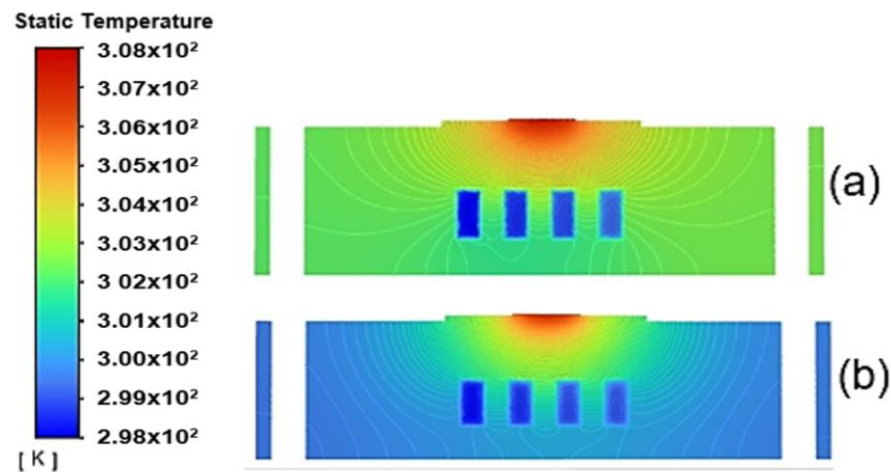
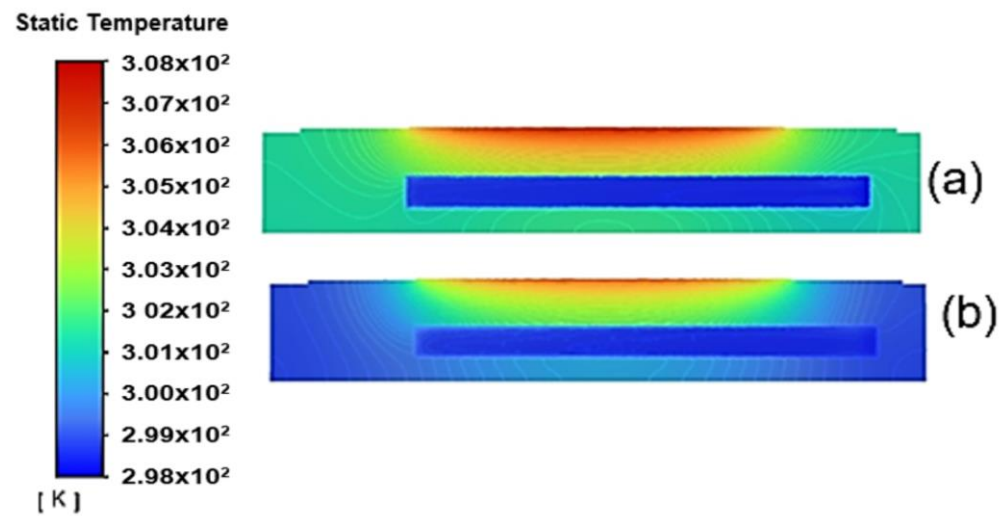


Figure 11. Temperature contour of x-y centre cut-view of the model from simulation (a) Continuous flow (b) Pulsating flow at 30 pulse/minute.

A 2D z-y centre channel cut-view temperature contour of the model for both continuous flow and pulsating flow at 1 L/m is shown in Figure 12, with maximum and minimum temperature intervals of 298 K to 308 K. Based on the temperature contour, it can be seen that the pulsating flow with a period of 2 s and a frequency of 0.5 Hz, which is equivalent to 30 pulses/minute (Figure 12b), shows better cooling compared to continuous flow (Figure 12a).



**Figure 12.** Temperature contour of z-y centre cut-view of the model from simulation (a) Continuous flow (b) Pulsating flow at 30 pulse/minute.

An overall coupled model temperature contour is shown in Figure 13, with a temperature interval of 298 K to 308 K. At a flow rate of 1 L/m, the comparison shows that the pulsating flow with a period of 2 s and a frequency of 0.5 Hz, equivalent to 30 pulses/min is more effective.

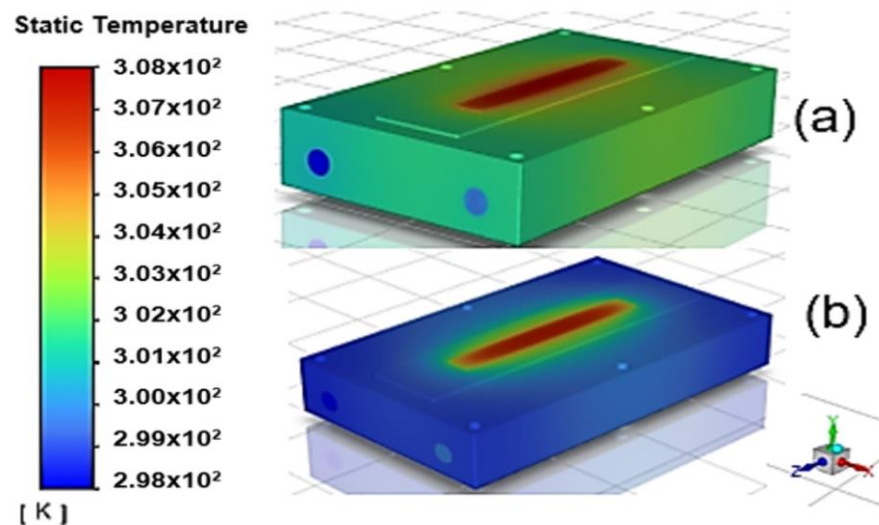


**Figure 13.** Temperature contour of the coupled model from simulation (a) Continuous flow (b) Pulsating flow at 30 pulse/minute.

Figure 14a shows the effect of coolant inlet temperature on the model. With an increase in the inlet temperature of the coolant from 298 K to 318 K, the solar cell and cooling pad temperature increased from 301.92898 K to 321.90656 K and 305.88118 K to 325.86523 K, respectively. In Figure 14b, the effect of the flow rate on the Reynolds number (Re) and the Nusselt number (Nu). An increase in flow rate increases the Re number. With an increase in flow rate from 0.5 L/m to 2.5 L/m, the Re with continuous flow increased from 1482.41 to 8372.26. While with the pulsating flow at 30 pulses/minutes, the Re increased from 1047.33 to 27,108.48. The Nusselt number increases with the Reynolds number in continuous and pulsating flow, which agrees with [13].



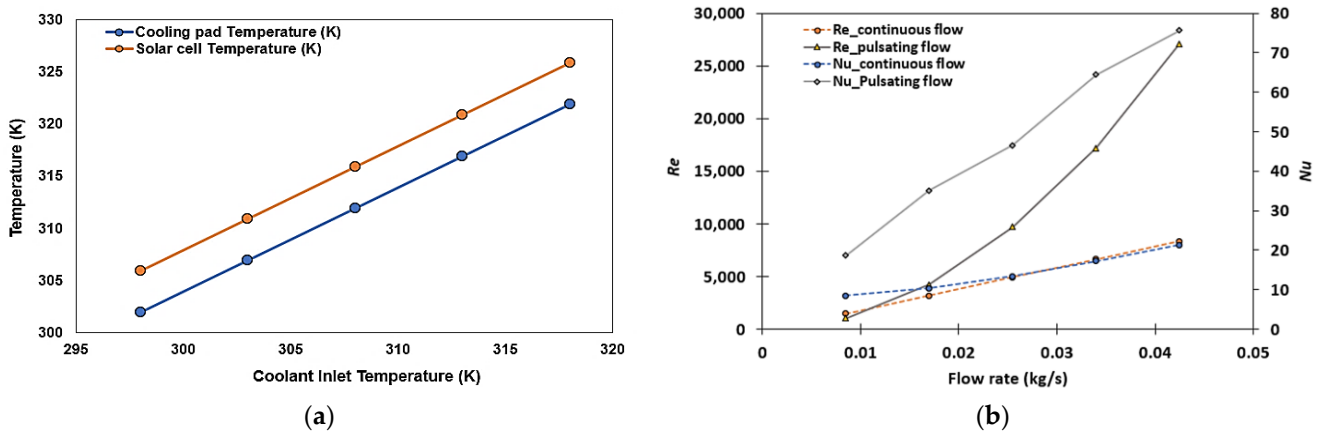


**Figure 14.** (a) Effect of inlet temperature on solar cell and cooling pad temperature (b) Reynolds number and Nusselt number versus flow rate.

Figure 15 illustrates the relationship between the Womersley number ( $\alpha$ ), the heat transfer rate, and the instantaneous velocity (U-p). The Womersley number indicates whether the uneven fluid flow in pulsing flow is almost constant. The Womersley number increases from 10.247 to 10.426 when the instantaneous velocity (U-p) increases from 0.14 to 0.73 m per second. The Womersley indicates that the pulsating flow is associated with the plug-like flow. Thus, the velocity profile is less than the pulse frequency. The enhancement in heat transmission increased from 2.196 to 3.539. Despite the increase in flow rate from 0.5 L/m to 2.5 L/m (Figure 15), at a speed of 0.587 m/s, the most significant improvement was seen. Hence, the pulsating flow made the cooling more effective and improved it by 37.95%.

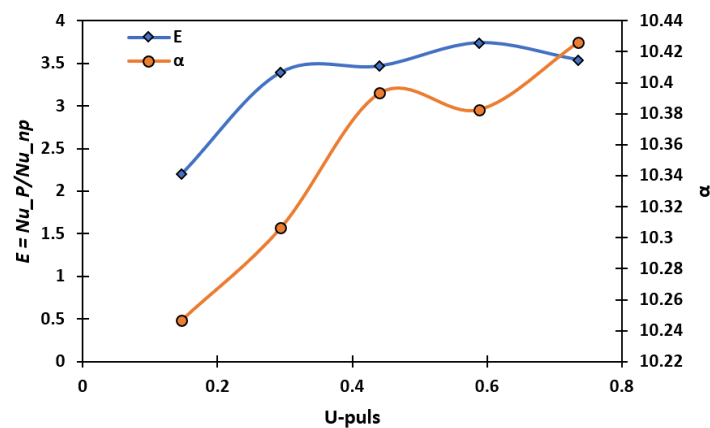


**Figure 15.** Pulsating velocity variation at  $T = 2$  s and  $f = 0.5$  Hz with cooling enhancement and Womersley number.

5.2. Experiment Results

Figure 16a demonstrates the effect of flow rate on the Reynolds number (Re) and Nusselt number (Nu). With an increase in flow rate from 0.5 L/m to 2.5 L/m, the Re with continuous flow increased from 1617.55 to 8341.65. With pulsating flow at 30 pulses/minutes, Re increased from 1025.24 to 32,251.15. The Nusselt number increases with the Reynolds number in continuous and pulsating flows, consistent with [88]. In Figure 16b, the relationship between the Womersley number ( $\alpha$ ) and the rate of heat transfer and instantaneous velocity (U-p) is illustrated. The Womersley number indicates whether the uneven fluid flow in pulsating flow is nearly constant. When the instantaneous velocity (U-p) increases from 0.14 m/s to 0.73 m/s, the Womersley number increase from 10.13 to 11.37. This Womersley number means that pulsating flow is associated with plug-like flow at the maximum, resulting in a velocity profile lower than the pulse frequency. The enhancement in heat

transmission fluctuates with maximum and minimum values of 12.21 and 9.02, respectively. At a speed of 0.73 m/s, the most significant improvement was observed.

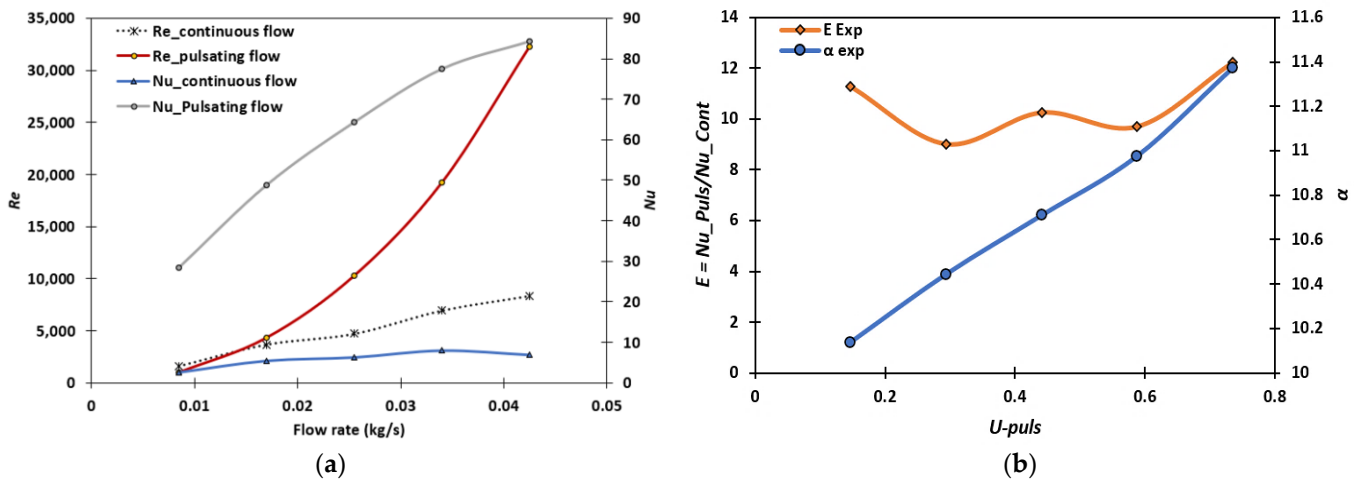


**Figure 16.** (a) Reynolds number and Nusselt number versus flow rate (b) Pulsating velocity variation at  $T = 2$  s and  $f = 0.5$  Hz with cooling enhancement and Womersley number.

Figure 17 shows the solar cell temperature against the flow rate for simulation and experiment. The cell temperature decreased with an increased flow rate in both the simulation and experiment. Several researchers have reported that an increased flow rate decreases cell temperature [68]. Similarly, in this research, the cell temperature drops from 307.25 K to 304.25 K with continuous flow when the flow rate increases from 0.5 L/m to 2.5 L/m. At the same time, with the pulsating flow at 30 pulses/minute, the cell temperature drops from 303.75 K to 303.2 K. This shows that the cell temperature is lower with the pulsating flow than with the continuous flow temperature. The temperature difference occurs because the simulation was conducted based on the assumption that the flow does not involve radiation heat transfer (ambient temperature). In reality, the temperature of the solar cell depends on factors such as ambient temperature. This factor could only be controlled to a certain extent in the experiment.

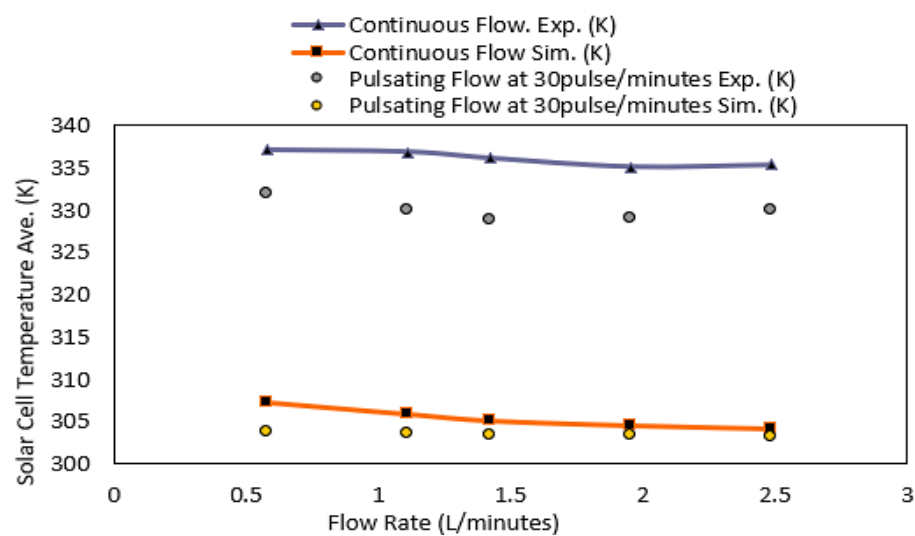


**Figure 17.** Solar cell temperature versus flow rate for continuous and pulsating flow at 30 pulse/min.

The experiment with pulsating flow starts to increase from 1.5 L/m to 2.5 L/m. This keeps the cell average output power constant from a 1.5 L/m to a 1.75 L/m flow rate (Figure 18). The increase in cell temperature is due to the extensive vibration experienced

during the pulsating flow experiment approach adopted in this research. The vibration became more intense as the flow rate increased from 0.5 L/m to 2.5 L/m. Additionally, the vibration becomes more intense between 1.5 L/m and 2.5 L/m, which leads to cracks on the temperature sensor holders, as indicated with a red circle in Figure 18. This results in leakage and affects the pulsating flow's cooling capability during the experiment between 2 L/m and 5 L/m. The system's vibration has been highlighted as a challenge in applying pulsating flow [90,102]. This challenge and a more detailed and efficient approach to pulsating flow with CPV cooling would be an area to explore in the next stage of this research.

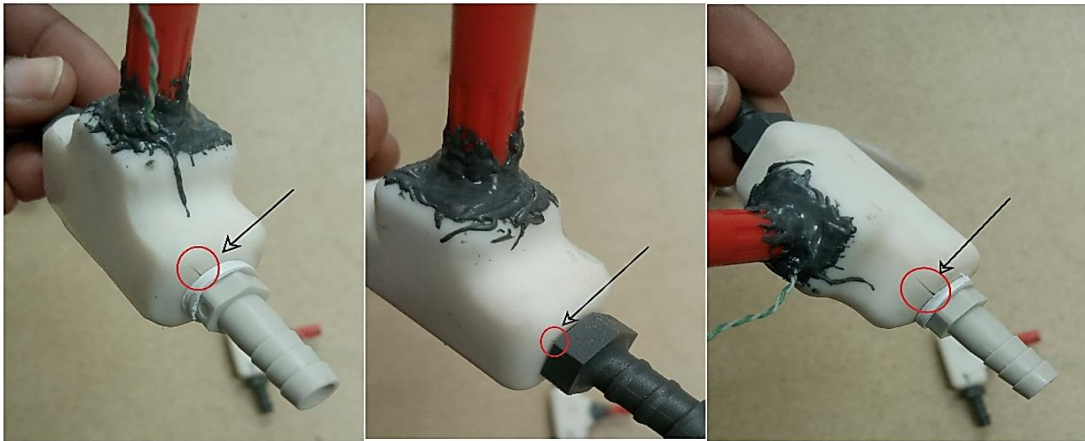


**Figure 18.** Cracks on temperature sensor holder due to pulsating flow at 30 pulse/min.

Figure 19 shows the solar cell output power versus coolant flow rate and cell temperature obtained during the experiments. With an increase in flow rate from 0.5 to 2.5 L/m, the solar cell power output increases for both continuous and pulsating flow, which agrees with [68]. The cell's pulsating flow power output shows better cooling than the continuous flow. However, it declines from 1.803 W to 1.792 W between 1.5 L/m and 2.5 L/m flow rate due to cell temperature increases caused by the overall system vibration, resulting in cracks and leakage in the inlet temperature sensors (Figure 18). Another factor that influences the decrease in power output and cell temperature increases is the ambient temperature, which rises from 403.143 K to 407.996 K due to the sun's concentration for more than 35 min. Uncontrollable factors such as ambient environmental temperature directly affect the performance of the heat sink and the solar cell.

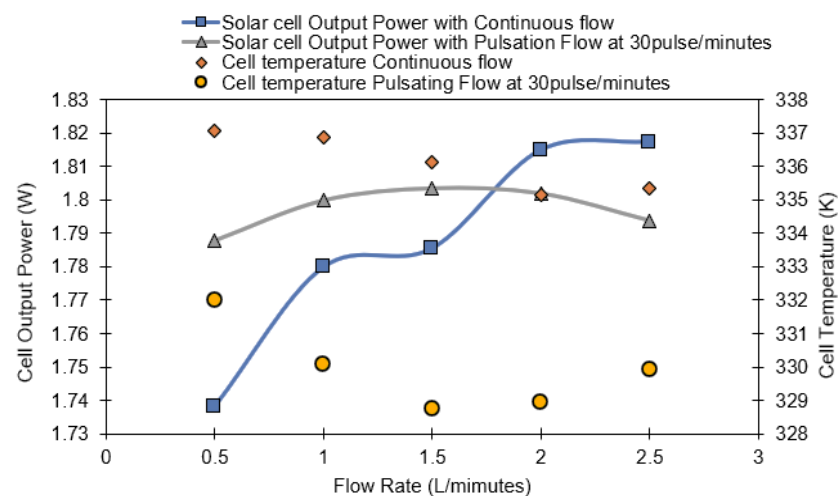


**Figure 19.** Solar cell output power and cell temperature versus flow rate.

### 5.3. Validation

Figure 20a shows the pressure drops for both the experiment and simulation. Although it is not the same, both simulation and experiments agree. The pressure drop was calculated using Equation (14). With an increase in flow rate from 0.5 L/m to 2.5 L/m, the pressure drops increase from 1940.28 Pa to 35,240.40 Pa and 1896.30 Pa to 34,961.30 Pa for simulation and experiment, respectively. This agrees with [68], where it was reported that with an increase in flow rate, pressure drop increases. Figure 19b shows the flow rate's effect on the Reynolds number (Re) for both simulation and experiment. As expected, an increase in flow rate increases the Re. With an increase in flow rate from 0.5 L/m to 2.5 L/m, the Re increased from 1617.56 to 8341.66 and 1482.41 to 8372.26 for experiment and simulation, respectively.

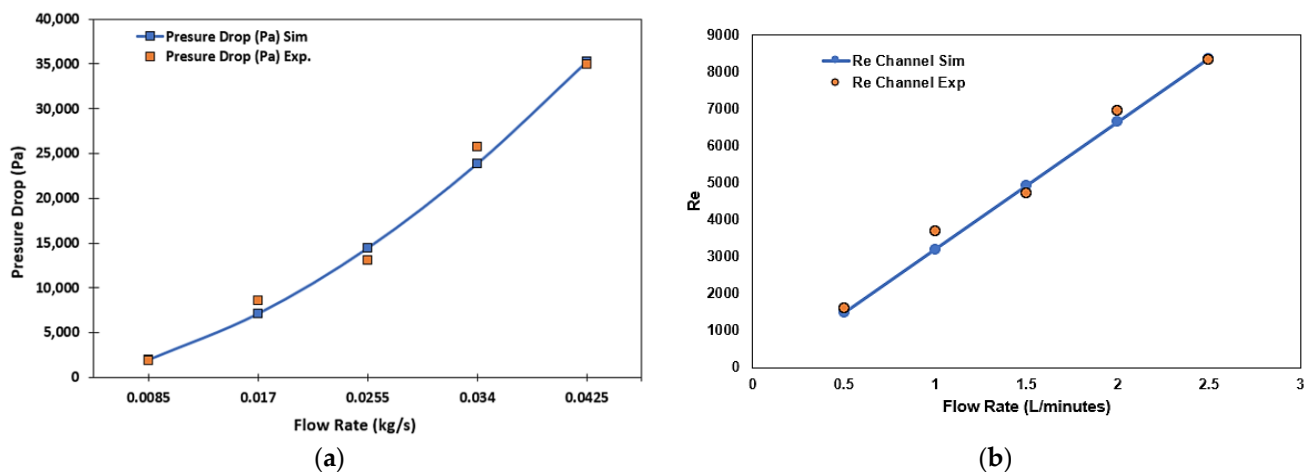


Figure 20. (a) Validation pressure drops versus flow rate (b) Reynolds number versus flow rate.

## 6. Future Work

Current research on CPV cooling is a challenging area. Several studies have highlighted concentrated solar cell temperature non-uniformity, resulting in hot regions and cooled spots that need further study: cell performance duration, pressure drop, liquid type, weight, and design limit immersion cooling. Impinging jets poses the challenge of temperature non-uniformity, spent fluid, and design complexity. Overheating, reverse thermal flows, and area-dependent cooling issues are challenges for heat pipe cooling systems. Limits on energy storage, mass weight dependent on cooling capacity, and utilisation of low-quality heat sources are limitations of phase change materials. Microchannel cooling has fundamental limitations such as pressure drops, corrosion, temperature non-uniformity along the channel, higher manufacturing costs, and higher power consumption.

Another challenge is the continuous fluctuation of solar radiation intensity due to uncontrollable conditions such as clouds. This is a challenge as our environment changes depending on the weather and cloud coverage. The sun's intensity concentrated on solar cells changes continuously, and the heat flux generated by the CPV also changes. The sudden fluctuation necessitates a more efficient approach to CPV cooling and increases the chances of temperature non-uniformity. This article has introduced a new approach to applying a pulsating flow to CPV cooling. The results of pulsating flow cooling in both simulation and experiments have proven to be efficient compared to continuous flow. However, the pulsating flow comes with a vibration challenge that affects the overall system performance. An area to focus on would be designing a system flow that minimises or eliminates system vibration with the pulsating flow. Future research should test different pulsating frequencies to optimise the system. CPV cooling with the pulsating flow, integrated with PCM or porous media, is worth investigating. An investigation using an optimised design with nanofluid instead of water as a coolant is an area to explore for pulsating flow CPV cooling.

Based on all the reviewed articles, applying a direct pulsating flow approach to cooling CPV has not been studied. A similar approach using control valves connected with a microcontroller to control the pulsating flow is possible with CPV cooling. This will allow additional control parameters to enhance heat transfer, apart from the flow rate. Applying a sensor to a part of the solar cell will cool the part at a higher temperature by pumping most of the coolant to that area. This will result in not utilising the coolant in an area where cooling is not required and channelling it to areas where cooling is required within the cell, thereby increasing uniformity. Additionally, this will reduce the amount of coolant used in CPV cooling and increase performance because the coolant is utilised in the area that requires the cooling most.

## 7. Conclusions

In conclusion, current techniques for cooling concentrated photovoltaic (CPV) panels are based on a continuous flow subjected to non-uniform temperature distribution issues throughout the cell. This article has reviewed various CPV cooling methods, focusing on the most applied techniques based on recently published research. The review shows that the direct coupled pulsating flow approach to CPV cooling has not been studied and presents an innovative approach using pulsating flow. Both simulation and experimental findings show that applying pulsating flow to current CPV cooling techniques is possible and more efficient than the conventional continuous flow. However, the pulsation vibration experienced during the experiment is a challenge that needs to be addressed. Future research can focus on exploring this area and designing a system flow that minimises or eliminates system vibration with the pulsating flow. A direct pulsating flow approach using control valves connected to a microcontroller can allow additional control parameters to enhance heat transfer apart from the flow rate. Furthermore, applying a sensor to a part of the solar cell can channel coolant to areas that require cooling most, increasing uniformity and reducing coolant usage. This article provides a new approach to efficient CPV cooling that warrants further exploration and research.

**Author Contributions:** Conceptualisation, K.A.I. and P.L.; methodology, K.A.I. and P.L.; software, K.A.I. and P.L.; validation, K.A.I. and P.L.; formal analysis, K.A.I.; investigation, K.A.I. and P.L.; resources, K.A.I., P.L. and Z.L.; data curation, K.A.I.; writing—original draft preparation, K.A.I. and P.L.; writing—review and editing, K.A.I., P.L. and Z.L.; supervision, P.L. All authors have read and agreed to the published version of the manuscript.

**Funding:** This studentship of the first author was funded by the Petroleum Technology Development Fund Nigeria through the 2020 scholarship award. The resources were partly funded by EPSRC, UK, under project reference EP/T006315/1.

**Data Availability Statement:** Data are contained within the article.

**Acknowledgments:** Special thanks to Fergus Crawley and Adriana Stawiarska.

**Conflicts of Interest:** The authors declared no conflict of interest.

## References

1. Gul, M.; Kotak, Y.; Muneer, T. Review on Recent Trend of Solar Photovoltaic Technology. *Energy Explor. Exploit.* **2016**, *34*, 485–526. [[CrossRef](#)]
2. Ankit; Sahoo, S.K.; Sukchai, S.; Yanine, F.F. Review and Comparative Study of Single-Stage Inverters for a PV System. *Renew. Sustain. Energy Rev.* **2018**, *91*, 962–986. [[CrossRef](#)]
3. Zhang, J.; Xuan, Y. Performance Improvement of a Photovoltaic—Thermoelectric Hybrid System Subjecting to Fluctuant Solar Radiation. *Renew. Energy* **2017**, *113*, 1551–1558. [[CrossRef](#)]
4. Al-Nimr, M.A.; Bukhari, M.; Mansour, M. A Combined CPV/T and ORC Solar Power Generation System Integrated with Geothermal Cooling and Electrolyser/Fuel Cell Storage Unit. *Energy* **2017**, *133*, 513–524. [[CrossRef](#)]
5. Abdulmunem, A.R.; Samin, P.M.; Rahman, H.A.; Hussien, H.A.; Mazali, I.I. Enhancing PV Cell's Electrical Efficiency Using Phase Change Material with Copper Foam Matrix and Multi-Walled Carbon Nanotubes as Passive Cooling Method. *Renew. Energy* **2020**, *160*, 663–675. [[CrossRef](#)]



6. Nandurkar, Y.; Shrivastava, R.L.; Soni, V.K. Improvement in Energy Efficiency of CPV Module by Way of Various Active and Passive Cooling Techniques. *J. Inst. Eng. India Ser. C* **2022**, *103*, 259–265. [[CrossRef](#)]
7. Sharaf, M.; Huzayyin, A.S.; Yousef, M.S. Performance Enhancement of Photovoltaic Cells Using Phase Change Material (PCM) in Winter. *Alex. Eng. J.* **2022**, *61*, 44. [[CrossRef](#)]
8. Xu, H.; Wang, N.; Zhang, C.; Qu, Z.; Karimi, F. Energy Conversion Performance of a PV/T-PCM System under Different Thermal Regulation Strategies. *Energy Convers. Manag.* **2021**, *229*, 113660. [[CrossRef](#)]
9. Ranabhat, K.; Patrikeev, L.; Revina, A.A.; Andrianov, K.; Lapshinsky, V.; Sofronova, E. An Introduction to Solar Cell Technology. *J. Appl. Eng. Sci.* **2016**, *14*, 481–491. [[CrossRef](#)]
10. Skullong, S.; Promvong, P.; Thianpong, C.; Pimsarn, M. Heat Transfer and Turbulent Flow Friction in a Round Tube with Staggered-Winglet Perforated-Tapes. *Int. J. Heat Mass Transf.* **2016**, *95*, 7. [[CrossRef](#)]
11. Singh, S.; Singh, S.K.; Mali, H.S.; Dayal, R. Numerical Investigation of Heat Transfer in Structured Rough Microchannels Subjected to Pulsed Flow. *Appl. Eng.* **2021**, *197*, 117361. [[CrossRef](#)]
12. Akdag, U.; Akcay, S.; Demiral, D. Heat Transfer Enhancement with Laminar Pulsating Nanofluid Flow in a Wavy Channel. *Int. Commun. Heat Mass Transf.* **2014**, *59*, 8. [[CrossRef](#)]
13. Naphon, P.; Wiriyasart, S. Experimental Study on Laminar Pulsating Flow and Heat Transfer of Nanofluids in Micro-Fins Tube with Magnetic Fields. *Int. J. Heat Mass Transf.* **2018**, *118*, 131. [[CrossRef](#)]
14. Kim, S.Y.; Kang, B.H.; Hyun, J.M. Heat Transfer from Pulsating Flow in a Channel Filled with Porous Media. *Int. J. Heat Mass Transf.* **1994**, *37*, 2025–2033. [[CrossRef](#)]
15. Huang, X.; Li, P.; Tan, Y. Time-Dependent Heat Transfer Analysis of Ellipsoidal Protruded Microchannel with Multiple Pulsating Jets. *Appl. Eng.* **2022**, *210*, 118348. [[CrossRef](#)]
16. Zhang, L.; Tian, L.; Zhang, A.; Chen, H. Effects of the Shape of Tube and Flow Field on Fluid Flow and Heat Transfer. *Int. Commun. Heat Mass Transf.* **2020**, *117*, 104782. [[CrossRef](#)]
17. Aghenta, L.O.; Iqbal, M.T. Development of an IoT Based Open Source SCADA System for PV System Monitoring. In Proceedings of the IEEE Canadian Conference of Electrical and Computer Engineering, CCECE 2019, Edmonton, AB, Canada, 5–8 May 2019.
18. Singh, B.P.; Goyal, S.K.; Kumar, P. Solar Pv Cell Materials and Technologies: Analysing the Recent Developments. *Proc. Mater. Today Proc.* **2021**, *2021*, 43. [[CrossRef](#)]
19. Abo-Zahhad, E.M.; Ookawara, S.; Radwan, A.; El-Shazly, A.H.; Elkady, M.F. Thermal and Structure Analyses of High Concentrator Solar Cell under Confined Jet Impingement Cooling. *Energy Convers. Manag.* **2018**, *176*, 39–54. [[CrossRef](#)]
20. Abo-Zahhad, E.M.; Ookawara, S.; Esmail, M.F.C.; El-Shazly, A.H.; Elkady, M.F.; Radwan, A. Thermal Management of High Concentrator Solar Cell Using New Designs of Stepwise Varying Width Microchannel Cooling Scheme. *Appl. Eng.* **2020**, *172*, 115124. [[CrossRef](#)]
21. Abo-Zahhad, E.M.; Ookawara, S.; Radwan, A.; El-Shazly, A.H.; El-Kady, M.F.; Esmail, M.F.C. Performance, Limits, and Thermal Stress Analysis of High Concentrator Multijunction Solar Cell under Passive Cooling Conditions. *Appl. Eng.* **2020**, *164*, 114497. [[CrossRef](#)]
22. Du, B.; Hu, E.; Kolhe, M. Performance Analysis of Water Cooled Concentrated Photovoltaic (CPV) System. *Renew. Sustain. Energy Rev.* **2012**, *16*, 6732–6736. [[CrossRef](#)]
23. Ahmed, A.; Shanks, K.; Sundaram, S.; Mallick, T. Energy and Exergy Analyses of New Cooling Schemes Based on a Serpentine Configuration for a High Concentrator Photovoltaic System. *Appl. Eng.* **2021**, *199*, 117528. [[CrossRef](#)]
24. Mallick, T.K.; Eames, P.C.; Norton, B. Using Air Flow to Alleviate Temperature Elevation in Solar Cells within Asymmetric Compound Parabolic Concentrators. *Sol. Energy* **2007**, *81*, 3. [[CrossRef](#)]
25. Hersh, P.; Zweibel, K.S. *Basic Photovoltaic Principles and Methods*; Energy Research Institute: Washington, DC, USA, 1982.
26. Nayan, M.F.; Ullah, S.M.S.; Saif, S.N. Comparative Analysis of PV Module Efficiency for Different Types of Silicon Materials Considering the Effects of Environmental Parameters. In Proceedings of the 3rd International Conference on Electrical Engineering and Information and Communication Technology, iCEEiCT 2016, Dhaka, Bangladesh, 22–24 September 2016.
27. Wilson, G.M.; Al-Jassim, M.; Metzger, W.K.; Glunz, S.W.; Verlinden, P.; Xiong, G.; Mansfield, L.M.; Stanbery, B.J.; Zhu, K.; Yan, Y.; et al. The 2020 Photovoltaic Technologies Roadmap. *J. Phys. D Appl. Phys.* **2020**, *53*, 493001. [[CrossRef](#)]
28. Itten, R.; Stucki, M. Highly Efficient 3rd Generation Multi-Junction Solar Cells Using Silicon Heterojunction and Perovskite Tandem: Prospective Life Cycle Environmental Impacts. *Energy* **2017**, *10*, 841. [[CrossRef](#)]
29. Philipps, S.P.; Bett, A.W. III-V Multi-Junction Solar Cells and Concentrating Photovoltaic (CPV) Systems. *Adv. Opt. Technol.* **2014**, *3*, 469–478. [[CrossRef](#)]
30. Ibrahim, K.A.; Kim, M.; Kinuthia, D.; Hussaini, Z.A.; Crawley, F.; Luo, Z. High Performance Green Hydrogen Generation System. In Proceedings of the IEEE 20th International Conference on Micro and Nanotechnology for Power Generation and Energy Conversion Applications, PowerMEMS 2021, Virtual, 6–8 December 2021.
31. Xiao, M.; Tang, L.; Zhang, X.; Lun, I.; Yuan, Y. A Review on Recent Development of Cooling Technologies for Concentrated Photovoltaics (CPV) Systems. *Energy* **2018**, *11*, 3416. [[CrossRef](#)]
32. Bahaidarah, H.M.S.; Baloch, A.A.B.; Gandhidasan, P. Uniform Cooling of Photovoltaic Panels: A Review. *Renew. Sustain. Energy Rev.* **2016**, *57*, 1520–1544. [[CrossRef](#)]
33. Sharaf, M.; Yousef, M.S.; Huzayyin, A.S. Review of Cooling Techniques Used to Enhance the Efficiency of Photovoltaic Power Systems. *Environ. Sci. Pollut. Res.* **2022**, *29*, 26131–26159. [[CrossRef](#)]

34. Wang, S.; Shi, J.; Chen, H.H.; Schafer, S.R.; Munir, M.; Stecker, G.; Pan, W.; Lee, J.J.; Chen, C.L. Cooling Design and Evaluation for Photovoltaic Cells within Constrained Space in a CPV/CSP Hybrid Solar System. *Appl. Eng.* **2017**, *110*, 196. [[CrossRef](#)]
35. Royne, A.; Dey, C.J.; Mills, D.R. Cooling of Photovoltaic Cells under Concentrated Illumination: A Critical Review. *Sol. Energy Mater. Sol. Cells* **2005**, *86*, 451–483. [[CrossRef](#)]
36. Tonui, J.K.; Tripanagnostopoulos, Y. Air-Cooled PV/T Solar Collectors with Low Cost Performance Improvements. *Sol. Energy* **2007**, *81*, 2. [[CrossRef](#)]
37. Radziemska, E. Performance Analysis of a Photovoltaic-Thermal Integrated System. *Int. J. Photoenergy* **2009**, *2009*, 732093. [[CrossRef](#)]
38. Anand, S.; Senthil Kumar, M.; Balasubramanian, K.R.; Ajith Krishnan, R.; Maheswari, L. An Experimental Study on Thermal Management of Concentrated Photovoltaic Cell Using Loop Heat Pipe and Heat Sink. *Heat Transf. Asian Res.* **2019**, *48*, 21504. [[CrossRef](#)]
39. Theristis, M.; Sarmah, N.; Mallick, T.K.; O'Donovan, T.S. Design and Numerical Analysis of Enhanced Cooling Techniques for a High Concentration Photovoltaic (HCPV) System. In Proceedings of the 27th European Photovoltaic Solar Energy Conference and Exhibition, Frankfurt, Germany, 24–28 September 2012.
40. Cui, M.; Chen, N.; Yang, X.; Wang, Y.; Bai, Y.; Zhang, X. Thermal Analysis and Test for Single Concentrator Solar Cells. *J. Semicond.* **2009**, *30*, 044011. [[CrossRef](#)]
41. Xu, J.; Luo, E.; Hochgreb, S. A Thermoacoustic Combined Cooling, Heating, and Power (CCHP) System for Waste Heat and LNG Cold Energy Recovery. *Energy* **2021**, *227*, 20341. [[CrossRef](#)]
42. Al-Amri, F.; Maatallah, T.S.; Al-Amri, O.F.; Ali, S.; Ali, S.; Ateeq, I.S.; Zachariah, R.; Kayed, T.S. Innovative Technique for Achieving Uniform Temperatures across Solar Panels Using Heat Pipes and Liquid Immersion Cooling in the Harsh Climate in the Kingdom of Saudi Arabia. *Alex. Eng. J.* **2022**, *61*, 1413–1424. [[CrossRef](#)]
43. Anderson, W.G.; Dussinger, P.M.; Sarraf, D.B.; Tamanna, S. Heat Pipe Cooling of Concentrating Photovoltaic Cells. In Proceedings of the Conference Record of the IEEE Photovoltaic Specialists Conference, San Diego, CA, USA, 11–16 May 2008.
44. Gilmore, N.; Timchenko, V.; Menictas, C. Microchannel Cooling of Concentrator Photovoltaics: A Review. *Renew. Sustain. Energy Rev.* **2018**, *90*, 1041–1059. [[CrossRef](#)]
45. Shittu, S.; Li, G.; Zhao, X.; Akhlaghi, Y.G.; Ma, X.; Yu, M. Comparative Study of a Concentrated Photovoltaic-Thermoelectric System with and without Flat Plate Heat Pipe. *Energy Convers. Manag.* **2019**, *193*, 55. [[CrossRef](#)]
46. Shittu, S.; Li, G.; Zhao, X.; Zhou, J.; Ma, X.; Akhlaghi, Y.G. Experimental Study and Exergy Analysis of Photovoltaic-Thermoelectric with Flat Plate Micro-Channel Heat Pipe. *Energy Convers. Manag.* **2020**, *207*, 112515. [[CrossRef](#)]
47. Badr, F.; Radwan, A.; Ahmed, M.; Hamed, A.M. An Experimental Study of the Concentrator Photovoltaic/Thermoelectric Generator Performance Using Different Passive Cooling Methods. *Renew. Energy* **2022**, *185*, 80. [[CrossRef](#)]
48. Han, X.; Lv, Y. Design and Dynamic Performance of a Concentrated Photovoltaic System with Vapor Chambers Cooling. *Appl. Eng.* **2022**, *201*, 117824. [[CrossRef](#)]
49. Han, X.; Zhao, X.; Chen, X. Design and Analysis of a Concentrating PV/T System with Nanofluid Based Spectral Beam Splitter and Heat Pipe Cooling. *Renew. Energy* **2020**, *162*, 131. [[CrossRef](#)]
50. Senthilkumar, M.; Balasubramanian, K.R.; Kottala, R.K.; Sivapirakasam, S.P.; Maheswari, L. Characterization of Form-Stable Phase-Change Material for Solar Photovoltaic Cooling. *J. Anal. Calorim.* **2020**, *141*, 2487–2496. [[CrossRef](#)]
51. Nasef, H.A.; Nada, S.A.; Hassan, H. Integrative Passive and Active Cooling System Using PCM and Nanofluid for Thermal Regulation of Concentrated Photovoltaic Solar Cells. *Energy Convers. Manag.* **2019**, *199*, 12065. [[CrossRef](#)]
52. Duan, J. A Novel Heat Sink for Cooling Concentrator Photovoltaic System Using PCM-Porous System. *Appl. Eng.* **2021**, *186*, 116522. [[CrossRef](#)]
53. Rahmanian, S.; Rahmanian-Koushkaki, H.; Omidvar, P.; Shahsavari, A. Nanofluid-PCM Heat Sink for Building Integrated Concentrated Photovoltaic with Thermal Energy Storage and Recovery Capability. *Sustain. Energy Technol. Assess.* **2021**, *46*, 101223. [[CrossRef](#)]
54. Aslfattahi, N.; Saidur, R.; Arifuzzaman, A.; Abdelrazik, A.S.; Samylingam, L.; Sabri, M.F.M.; Sidik, N.A.C. Improved Thermo-Physical Properties and Energy Efficiency of Hybrid PCM/Graphene-Silver Nanocomposite in a Hybrid CPV/Thermal Solar System. *J. Anal. Calorim.* **2022**, *147*, 125–1142. [[CrossRef](#)]
55. Barrau, J.; Omri, M.; Chemisana, D.; Rosell, J.; Ibañez, M.; Tadríst, L. Numerical Study of a Hybrid Jet Impingement/Micro-Channel Cooling Scheme. *Appl. Eng.* **2012**, *33–34*, 1. [[CrossRef](#)]
56. Barrau, J.; Perona, A.; Dollet, A.; Rosell, J. Outdoor Test of a Hybrid Jet Impingement/Micro-Channel Cooling Device for Densely Packed Concentrated Photovoltaic Cells. *Sol. Energy* **2014**, *107*, 113–121. [[CrossRef](#)]
57. Awad, M.; Radwan, A.; Abdelrehim, O.; Emam, M.; Shmroukh, A.N.; Ahmed, M. Performance Evaluation of Concentrator Photovoltaic Systems Integrated with a New Jet Impingement-Microchannel Heat Sink and Heat Spreader. *Sol. Energy* **2020**, *199*, 78. [[CrossRef](#)]
58. Barrau, J.; Rosell, J.; Chemisana, D.; Tadríst, L.; Ibañez, M. Effect of a Hybrid Jet Impingement/Micro-Channel Cooling Device on the Performance of Densely Packed PV Cells under High Concentration. *Sol. Energy* **2011**, *85*, 4. [[CrossRef](#)]
59. Han, X.; Wang, Y.; Zhu, L. Electrical and Thermal Performance of Silicon Concentrator Solar Cells Immersed in Dielectric Liquids. *Appl. Energy* **2011**, *88*, 37. [[CrossRef](#)]

60. Mehrotra, S.; Rawat, P.; Debbarma, M.; Sudhakar, K. Performance of a Solar Panel with Water Immersion Cooling Technique. *Int. J. Sci. Environ. Technol.* **2014**, *3*, 1161–1172.
61. Rawat, P.; Sudhakar, K. Performance Analysis of Partially Covered Photovoltaic Thermal Water Collector. *Int. J. Res. Eng. Technol.* **2016**, *5*. [[CrossRef](#)]
62. Sun, Y.; Wang, Y.; Zhu, L.; Yin, B.; Xiang, H.; Huang, Q. Direct Liquid-Immersion Cooling of Concentrator Silicon Solar Cells in a Linear Concentrating Photovoltaic Receiver. *Energy* **2014**, *65*, 264–271. [[CrossRef](#)]
63. Kang, X.; Wang, Y.; Huang, Q.; Cui, Y.; Shi, X.; Sun, Y. Study on Direct-Contact Phase-Change Liquid Immersion Cooling Dense-Array Solar Cells under High Concentration Ratios. *Energy Convers. Manag.* **2016**, *128*, 73. [[CrossRef](#)]
64. Xin, G.; Wang, Y.; Sun, Y.; Huang, Q.; Zhu, L. Experimental Study of Liquid-Immersion III-V Multi-Junction Solar Cells with Dimethyl Silicon Oil under High Concentrations. *Energy Convers. Manag.* **2015**, *94*, 63. [[CrossRef](#)]
65. Farahani, S.D.; Alibeigi, M.; Zakinia, A.; Goodarzi, M. The Effect of Microchannel-Porous Media and Nanofluid on Temperature and Performance of CPV System. *J. Anal. Calorim.* **2021**, *147*, 7945–7962. [[CrossRef](#)]
66. Radwan, A.; Ookawara, S.; Ahmed, M. Analysis and Simulation of Concentrating Photovoltaic Systems with a Microchannel Heat Sink. *Sol. Energy* **2016**, *136*, 70. [[CrossRef](#)]
67. Soliman, A.M.A.; Hassan, H. Effect of Heat Spreader Size, Microchannel Configuration and Nanoparticles on the Performance of PV-Heat Spreader-Microchannels System. *Sol. Energy* **2019**, *182*, 59. [[CrossRef](#)]
68. Yang, K.; Zuo, C. A Novel Multi-Layer Manifold Microchannel Cooling System for Concentrating Photovoltaic Cells. *Energy Convers. Manag.* **2015**, *89*, 46. [[CrossRef](#)]
69. Sohel Murshed, S.M.; Nieto de Castro, C.A. A Critical Review of Traditional and Emerging Techniques and Fluids for Electronics Cooling. *Renew. Sustain. Energy Rev.* **2017**, *78*, 821–833. [[CrossRef](#)]
70. Ghani, I.A.; Sidik, N.A.C.; Kamaruzaman, N. Hydrothermal Performance of Microchannel Heat Sink: The Effect of Channel Design. *Int. J. Heat Mass Transf.* **2017**, *107*, 21–44. [[CrossRef](#)]
71. Bhandari, P.; Singh, J.; Kumar, K.; Ranakoti, L. A review on active techniques in microchannel heat sink for miniaturisation problem in electronic industry. *Acta Innov.* **2022**, *2022*, 45–54. [[CrossRef](#)]
72. Ganguly, S.; Sarkar, S.; Kumar Hota, T.; Mishra, M. Thermally Developing Combined Electroosmotic and Pressure-Driven Flow of Nanofluids in a Microchannel under the Effect of Magnetic Field. *Chem. Eng. Sci.* **2015**, *126*, 60. [[CrossRef](#)]
73. Shit, G.C.; Mondal, A.; Sinha, A.; Kundu, P.K. Electro-Osmotically Driven MHD Flow and Heat Transfer in Micro-Channel. *Phys. A Stat. Mech. Appl.* **2016**, *449*, 8. [[CrossRef](#)]
74. Akachi Hisateru US 4921041 A—Structure of a Heat Pipe. Available online: <https://www.lens.org/lens/patent/151-789-425-811-172/frontpage> (accessed on 29 May 2022).
75. Faghri, A. Heat pipes: Review, opportunities and challenges. *Front. Heat Pipes* **2014**, *5*, 1. [[CrossRef](#)]
76. Nikolayev, V.S. Physical Principles and State-of-the-Art of Modeling of the Pulsating Heat Pipe: A Review. *Appl. Eng.* **2021**, *195*, 117111. [[CrossRef](#)]
77. Zhang, Y.; Faghri, A. Advances and Unsolved Issues in Pulsating Heat Pipes. *Heat Transf. Eng.* **2008**, *29*, 20–44. [[CrossRef](#)]
78. Khandekar, S.; Charoensawan, P.; Groll, M.; Terdtoon, P. Closed Loop Pulsating Heat Pipes—Part B: Visualisation and Semi-Empirical Modeling. *Appl. Therm. Eng.* **2003**, *23*, 2021–2033. [[CrossRef](#)]
79. Liu, X.; Sun, Q.; Zhang, C.; Wu, L. High-Speed Visual Analysis of Fluid Flow and Heat Transfer in Oscillating Heat Pipes with Different Diameters. *Appl. Sci.* **2016**, *6*, 321. [[CrossRef](#)]
80. Kim, J.; Kim, S.J. Experimental Investigation on Working Fluid Selection in a Micro Pulsating Heat Pipe. *Energy Convers. Manag.* **2020**, *205*, 112462. [[CrossRef](#)]
81. Kim, W.; Kim, S.J. Effect of Reentrant Cavities on the Thermal Performance of a Pulsating Heat Pipe. *Appl. Eng.* **2018**, *133*, 27. [[CrossRef](#)]
82. Kim, W.; Kim, S.J. Effect of a Flow Behavior on the Thermal Performance of Closed-Loop and Closed-End Pulsating Heat Pipes. *Int. J. Heat Mass Transf.* **2020**, *149*, 119251. [[CrossRef](#)]
83. Youn, Y.J.; Kim, S.J. Fabrication and Evaluation of a Silicon-Based Micro Pulsating Heat Spreader. *Sens. Actuators A Phys.* **2012**, *174*, 6. [[CrossRef](#)]
84. Elshafei, E.A.M.; Safwat Mohamed, M.; Mansour, H.; Sakr, M. Experimental Study of Heat Transfer in Pulsating Turbulent Flow in a Pipe. *Int. J. Heat Fluid Flow* **2008**, *29*, 18. [[CrossRef](#)]
85. Hemmat Esfe, M.; Bahiraei, M.; Torabi, A.; Valadkhani, M. A Critical Review on Pulsating Flow in Conventional Fluids and Nanofluids: Thermo-Hydraulic Characteristics. *Int. Commun. Heat Mass Transf.* **2021**, *120*, 104859. [[CrossRef](#)]
86. Yellin, E.L. Laminar-Turbulent Transition Process in Pulsatile Flow. *Circ. Res.* **1966**, *19*, 791–804. [[CrossRef](#)]
87. Yu, H.; Zhuang, J.; Li, T.; Li, W.; He, T.; Mao, N. Influence of Transient Heat Flux on Boiling Flow Pattern in a Straight Microchannel Applied in Concentrator Photovoltaic Systems. *Int. J. Heat Mass Transf.* **2022**, *190*, 122792. [[CrossRef](#)]
88. Alizadeh, H.; Ghasempour, R.; Shafii, M.B.; Ahmadi, M.H.; Yan, W.M.; Nazari, M.A. Numerical Simulation of PV Cooling by Using Single Turn Pulsating Heat Pipe. *Int. J. Heat Mass Transf.* **2018**, *127*, 108. [[CrossRef](#)]
89. Dang, S.N.; Xue, H.J.; Zhang, X.Y.; Qu, J.; Zhong, C.W.; Chen, S.Y. Three-Dimensional Human Thermoregulation Model Based on Pulsatile Blood Flow and Heating Mechanism. *Chin. Phys. B* **2018**, *27*, 114402. [[CrossRef](#)]
90. Ye, Q.; Zhang, Y.; Wei, J. A Comprehensive Review of Pulsating Flow on Heat Transfer Enhancement. *Appl. Eng.* **2021**, *196*, 117275. [[CrossRef](#)]

91. al Siyabi, I.; Shanks, K.; Mallick, T.; Sundaram, S. Indoor and Outdoor Characterization of Concentrating Photovoltaic Attached to Multi-Layered Microchannel Heat Sink. *Sol. Energy* **2020**, *202*, 55–72. [[CrossRef](#)]
92. Ahmed, H.E.; Ahmed, M.I.; Seder, I.M.F.; Salman, B.H. Experimental Investigation for Sequential Triangular Double-Layered Microchannel Heat Sink with Nanofluids. *Int. Commun. Heat Mass Transf.* **2016**, *77*, 104–115. [[CrossRef](#)]
93. Jiang, P.X.; Fan, M.H.; Si, G.S.; Ren, Z.P. Thermal-Hydraulic Performance of Small Scale Micro-Channel and Porous-Media Heat-Exchangers. *Int. J. Heat Mass Transf.* **2001**, *44*, 1039–1051. [[CrossRef](#)]
94. Olayiwola, B.O.; Schaldach, G.; Walzel, P. CFD Simulations of Flow and Heat transfer in a Zigzag channel with Flow Pulsation. *Int. Mech. Eng. Congr. Expo.* **2012**, *44*, 1531–1541.
95. Bayomy, A.M.; Saghir, M.Z. Heat Transfer Characteristics of Aluminum Metal Foam Subjected to a Pulsating/Steady Water Flow: Experimental and Numerical Approach. *Int. J. Heat Mass Transf.* **2016**, *97*, 9. [[CrossRef](#)]
96. Haibullina, A.; Khairullin, A.; Balzamor, D.; Ilyin, V.; Bronskaya, V.; Khairullina, L. Local Heat Transfer Dynamics in the In-Line Tube Bundle under Asymmetrical Pulsating Flow. *Energy* **2022**, *15*, 571. [[CrossRef](#)]
97. Tan, L.; Yuan, Y.; Huang, C. CFD Modelling on Flow Field Characteristics of Engine Cooling Water Jacket and Its Cooling Performance Improvement Based on Coolant Transport Path Analysis Method. *Proc. Inst. Mech. Eng. Part A J. Power Energy* **2022**, *237*, 385–401. [[CrossRef](#)]
98. Altaç, Z.; Mahir, N. A Comparative Assessment of Turbulent Forced Convection Heat Transfer from a Single Cylinder Using RANS and Les Models. *J. Therm. Sci. Technol.* **2018**, *38*, 11–24.
99. Afroz, F.; Sharif, M.A.R. Numerical Investigation of Heat Transfer from a Plane Surface Due to Turbulent Annular Swirling Jet Impingement. *Int. J. Therm. Sci.* **2020**, *151*, 106257. [[CrossRef](#)]
100. Montorfano, D.; Gaetano, A.; Barbato, M.C.; Ambrosetti, G.; Pedretti, A. CPV Cells Cooling System Based on Submerged Jet Impingement: CFD Modeling and Experimental Validation. In Proceedings of the AIP Conference Proceedings, Surakarta, Indonesia, 12 May 2014; Volume 1616.
101. Lee, S.S.; Lai, S.O.; Chong, K.K. A Study on Cooling of Concentrator Photovoltaic Cells Using CFD. In Proceedings of the ICIMTR 2012—2012 International Conference on Innovation, Management and Technology Research, Malacca, Malaysia, 21–22 May 2012.
102. Kurtulmuş, N.; Sahin, B. Experimental Investigation of Pulsating Flow Structures and Heat Transfer Characteristics in Sinusoidal Channels. *Int. J. Mech. Sci.* **2020**, *167*, 268. [[CrossRef](#)]

**Disclaimer/Publisher’s Note:** The statements, opinions and data contained in all publications are solely those of the individual author(s) and contributor(s) and not of MDPI and/or the editor(s). MDPI and/or the editor(s) disclaim responsibility for any injury to people or property resulting from any ideas, methods, instructions or products referred to in the content.